

UC San Diego

UC San Diego Previously Published Works

Title

Chemotropic guidance facilitates axonal regeneration and synapse formation after spinal cord injury.

Permalink

<https://escholarship.org/uc/item/9vs5w4kd>

Journal

Nature neuroscience, 12(9)

ISSN

1097-6256

Authors

Alto, Laura Taylor
Havton, Leif A
Conner, James M
et al.

Publication Date

2009-09-01

DOI

10.1038/nn.2365

Peer reviewed



Published in final edited form as:

Nat Neurosci. 2009 September ; 12(9): 1106–1113. doi:10.1038/nn.2365.

Chemotropic Guidance Facilitates Axonal Regeneration and Synapse Formation after Spinal Cord Injury

Laura Taylor Alto¹, Leif A. Havton², James M. Conner¹, Edmund R. Hollis II¹, Armin Blesch^{1,*}, and Mark H. Tuszynski^{1,3,*}

¹Department of Neurosciences, University of California, La Jolla, California 92093-0626

²Department of Neurology, University of California, Los Angeles, California 90095

³Veterans Administration Medical Center, San Diego, California 92165

Abstract

A principal objective of spinal cord injury (SCI) research is the restoration of axonal connectivity to denervated targets. We tested the hypothesis that chemotropic mechanisms would guide regenerating spinal cord axons to appropriate brainstem targets. Rats underwent cervical level 1 (C1) lesions followed by combinatorial treatments to elicit axonal bridging into and beyond lesion sites. Lentiviral vectors expressing neurotrophin-3 (NT-3) were then injected into an appropriate brainstem target, the nucleus gracilis, and an inappropriate target, the reticular formation. NT-3 expression in the correct target led to reinnervation of the nucleus gracilis in a dose-related fashion, whereas NT-3 expression in the reticular formation led to mistargeting of regenerating axons. Axons regenerating into the nucleus gracilis formed axodendritic synapses containing rounded vesicles, reflective of pre-injury synaptic architecture. Thus, we report for the first time the reinnervation of brainstem targets after SCI, and an essential role for chemotropic axon guidance in target selection.

Keywords

neurotrophin-3; spinal cord injury; ascending sensory; gene therapy; lentivirus; regeneration; reinnervation

INTRODUCTION

Functional deficits after spinal cord injury (SCI) are caused primarily by destruction of axonal connections between neurons and failure of spontaneous axonal regeneration. Regeneration failure is attributed to factors intrinsic to injured neurons, including the inability to activate genetic growth programs 1-4, and to extrinsic factors, including

Users may view, print, copy, and download text and data-mine the content in such documents, for the purposes of academic research, subject always to the full Conditions of use:http://www.nature.com/authors/editorial_policies/license.html#terms

*To whom correspondence should be addressed. Telephone: 858-534-8857 FAX: 858-534-5220 Email: mtuszynski@ucsd.edu ablesch@ucsd.edu.

Author roles: LA designed experiments, performed surgery, labeled tissue, analyzed data and wrote the manuscript; LH performed ultrastructural studies and analysis; JC performed electrophysiological analyses; EH examined myelination state of regenerated axons; AB and MHT designed experiments, performed surgery, analyzed data and wrote the manuscript.

molecular inhibitors 5. By systematically targeting these mechanisms, a number of experimental strategies promote either sprouting of spared axons, or regeneration of injured axons, within and beyond sites of SCI 6-11.

An unfulfilled goal of spinal cord regeneration research remains the reinnervation of natural neuronal targets. Target reinnervation has become a more prescient issue as individual and combined strategies for eliciting axonal regeneration succeed in promoting axonal growth beyond lesion sites. Once a regenerating axon emerges from a site of injury and encounters potential distal neuronal targets for reinnervation, will the axon locate an appropriate target among millions of potentially incorrect neuronal partners? Can guidance signals utilized during development, such as neurotrophic factors, also guide adult regenerating axons? Once axons reach a target, will they form synapses, do so at appropriate sites on postsynaptic neurons, and exhibit appropriate excitatory vs. inhibitory synaptic morphologies?

Recent progress in promoting bridging growth of dorsal column sensory axons after adult SCI provides an opportunity to test the hypothesis that developmentally-regulated guidance mechanisms will direct regenerating axons to appropriate targets and support new synapse formation in the adult CNS, and more specifically in a natural brainstem target. We recently reported that the combination of: 1) a cellular matrix placed in a lesion cavity, 2) a conditioning stimulus to the neuronal cell body, and 3) growth factor gradients beyond a lesion, succeed in promoting sensory axon regeneration into and beyond a C4 spinal cord lesion site 8, 10. Under these circumstances, axons regenerate distances of several millimeters, but remain 10 mm short of their natural target in the brainstem, the nucleus gracilis. In order to study mechanisms that direct axonal growth into targets, we placed spinal cord lesions at C1, an approximate two millimeter distance from the nucleus gracilis, establishing a paradigm whereby axons emerging from the graft encounter several gray matter neuronal groups as “choices” for growth in the caudal medulla (Fig. 1). These neuronal groups include the nucleus gracilis, an appropriate target, and the underlying medullary reticular formation, an inappropriate target. We then examined whether NT-3 would guide regenerating sensory axons into their appropriate target and support synapse formation.

We report that regenerating axons in the injured adult CNS utilized chemotropic mechanisms to direct growth beyond a lesion site and into an appropriate target. Further, axons regenerating into their natural adult target re-established appropriate axo-dendritic synapses with the host and adopted pre-injured patterns of asymmetric, excitatory synapses. Thus, regeneration into natural targets was experimentally induced after adult SCI.

RESULTS

Previous ELISA measurements established that injections of lentiviral vectors expressing NT-3 constitute a gradient of NT-3 protein that peaks at the site of vector injection, and progressively diminishes to undetectable levels 4 mm from the injection site 10. We therefore used lentiviral vectors to topographically express NT-3 in the brainstem to determine whether NT-3 could guide regenerating axons into specific targets beyond the

lesion. Animals underwent dorsal column lesions at C1 followed by grafting of autologous bone marrow stromal cells into the lesion site to provide a cellular “bridge” for regenerating axons 8, 10, 12 (Fig. 1). The retrogradely-transported tracer Fluorogold (FG) was injected into the thalamic ventroposterolateral nucleus, where axons projecting from the nucleus gracilis terminate, allowing identification of individual neuronal targets in the nucleus gracilis. After lesions and cell grafting, animals received injections of lentiviral vectors expressing either NT-3 or Green Fluorescent Protein (GFP, control) into the nucleus gracilis and the medullary reticular formation, providing two potential target sites for regenerating axons beyond the lesion. We employed sciatic nerve preconditioning lesions, which have been shown to promote axonal regeneration of ascending sensory axons, 8, 13-16 in combination with NT-3 delivery to elicit axon growth beyond the C1 lesion toward sites of NT-3 expression. Axonal regeneration was assessed based on cholera toxin B subunit (CTB) transganglionic labeling of injured dorsal column sensory axons 1 month after lesion/treatment.

The following groups were examined: 7 animals received conditioning lesions and injections of NT-3 lentiviral vectors (titer 100 µg/ml p24) into the nucleus gracilis and the medullary reticular formation (“Lenti-NT-3+CL”). 6 subjects received the same lenti-NT-3 injections, but no conditioning lesion (“Lenti-NT-3+NoCL”). 8 subjects received conditioning lesions and injections of GFP lentiviral vectors into the gracile and reticular nuclei (“Lenti-GFP+CL”); NT-3 was not provided. Finally, 9 animals received no conditioning lesion and lenti-GFP injections into both brainstem nuclei (“Lenti-GFP+NoCL”).

After obtaining preliminary results from the groups above, we added an additional group of “full treatment” subjects (conditioning lesions and lenti-NT-3 injection) (“Lenti-NT-3 high+CL”, 7 animals). In these animals, lenti-NT-3 vector was injected solely into the nucleus gracilis at a two-fold higher vector titer (200 µg/ml p24) to determine whether increased NT-3 expression in the nucleus gracilis would correspondingly increase sensory axonal regeneration into the appropriate target. Before analysis of axon regeneration, lesion completeness in all groups was assessed using conservative criteria (see Methods). To allow comparison between the intact nucleus gracilis and the nucleus gracilis after injury, 5 animals received CTB tracer injections, but no C1 lesion.

Combined Treatment Promotes Nucleus Gracilis Reinnervation

Immunohistochemistry for NT-3 indicated NT-3 expression in the nucleus gracilis only in animals that received lenti-NT-3 vectors (Supplementary Fig. 1). Animals that received NT-3 delivery to the brainstem exhibited sensory axon regeneration beyond the lesion site, whereas those that received GFP delivery did not (Figs. 2 and 3). Moreover, in the presence of lenti-NT-3 targeting to the nucleus gracilis, axons regenerated into this appropriate target (Fig. 2). Comparing the number of axon profiles in the nucleus gracilis between groups that received equivalent titers of lentiviral vectors, only full combinatorial treatment (Lenti NT-3+CL) promoted significantly greater axon growth into the target compared to controls (Figs. 3 and 4). Subjects receiving cell grafts and lenti-NT-3 injections into the nucleus gracilis without conditioning lesions (Lenti-NT-3+NoCL), had 2-fold fewer axonal profiles in the nucleus gracilis than combinatorially treated animals, and did not significantly differ

from controls (Figs. 3 and 4). Further, only half of all animals in the Lenti-NT-3+NoCL group exhibited bridging axons, whereas all subjects in the Lenti-NT-3+CL group exhibited bridging axons. Among control groups treated only with cell grafts and lenti-GFP injections (Lenti-GFP+noCL), axons did not extend beyond the lesion site or into the nucleus gracilis. In control subjects receiving lenti-GFP injections, cell grafts and conditioning lesions (Lenti-GFP+CL), only rare axons extended to the rostral host-graft interface, but none entered the nucleus gracilis (Figs. 3 and 4).

After establishing that full combinatorial treatment achieved significant regenerative axon growth into the target nucleus, we examined whether increasing NT-3 expression exclusively in the nucleus gracilis could further augment axon growth in combinatorially treated animals. In fact, animals that received full combinatorial treatment with high titer lenti-NT-3 vectors targeted solely to the nucleus gracilis (Lenti-NT-3 high+CL) exhibited significantly higher axon number in the target compared to animals that received combinatorial treatment with lower titer NT-3 vectors (Lenti-NT-3+CL, Figs. 3 and 4). Examination of reporter gene expression (lenti-NT-3 constructs express GFP via an internal ribosome entry site) confirmed that vector spread within the target significantly increased upon administration of the higher vector dose (Fig. 4). Thus, axons exhibited a dose-dependency to growth within the target.

To estimate the extent of axonal regrowth in lesioned/treated groups, the number of axon profiles in the nucleus gracilis was compared to intact animals (Figs. 3 and 4). Lenti-NT-3 high+CL treatment restored the number of axon profiles to 27% of values observed in the intact nucleus gracilis. Lenti-NT-3+CL restored 6.8% of axonal profiles, and Lenti-NT-3+NoCL restored only 3%. Thus, conditioning lesions plus chemotropic guidance achieved a relatively high degree of target re-penetration by regenerating axons.

NT-3 Guides Axons to Appropriate Brainstem Targets

Animals with NT-3 expression in the correct target, the nucleus gracilis, exhibited axonal growth throughout the nucleus. Regions of axonal growth precisely correlated with the topography of lenti-NT-3-GFP reporter gene expression in the target (Fig. 2). Animals that were subjected to NT-3 expression in the incorrect target, the medullary reticular formation, demonstrated axon growth in these ectopic regions of NT-3 expression (Fig. 5). In one case, lenti-NT-3 was mis-targeted 900 μ m rostral to the nucleus gracilis in the brainstem; in this subject, axons grew beyond the nucleus gracilis along the mis-targeted zone of lenti-NT-3 expression. In contrast, we did not observe ectopic axons in intact animals or among subjects in which lenti-NT-3 was expressed only in the nucleus gracilis. Thus, NT-3 specifically guided regenerating adult axons toward targets. These results demonstrate that axons regenerating after adult CNS injury exhibit classic directional and dose responsiveness to chemotropic gradients of growth factors.

Regenerating Sensory Axons Form Synapses in the Target

Confocal analysis demonstrated that regenerated CTB-labeled axons in the nucleus gracilis intimately associated with FG-labeled target neurons (Fig. 6a,b). To determine whether adult, injured axons re-formed synapses upon reaching their gracilar target, we analyzed the

nucleus gracilis by immuno-electron microscopy in two subjects receiving combinatorial treatment and high titer lenti-NT-3 delivery specifically to the nucleus gracilis (Lenti-NT-3 high+CL), and in three intact animals. 2-5 ultrathin sections per subject from the nucleus gracilis were screened for evidence of CTB-labeled axon terminals at 4800x magnification. Regenerating axon terminals were identified ultrastructurally by their electron-dense appearance, after immunohistochemical labeling for CTB and processing for streptavidin-HRP reaction product (Fig. 6c-e).

We identified a total of six CTB-labeled axon terminals ultrastructurally in two lesioned/combinatorially treated animals (2 in one subject, 4 in another), and 10 terminals in three intact animals. Each CTB-labeled axon terminal in lesioned/combinatorially treated animals contained specializations with ultrastructural features of synapses (Fig. 6c,d). Regenerated terminals exhibited formation of asymmetric synaptic specializations with a prominent postsynaptic element, typical of excitatory synapses 17, 18. Dense clusters of synaptic vesicles were evident in these terminal regions, indicating formation of functional structures required for neurotransmitter storage and release. Boutons in regenerated CTB-labeled axon terminals contained round rather than flattened synaptic vesicles, further suggesting an excitatory neurotransmitter phenotype 19. Four of the six regenerating axon terminals studied made synaptic contacts with multiple dendritic targets, a common feature for primary afferent projections to the gracile nucleus in intact rats 20, 21 (see below); the remaining two terminals made synaptic contact with single dendritic targets. Finally, CTB-containing regenerating axon terminals made synaptic contacts with dendritic rather than somal elements, a feature typical of the pre-injury ultrastructural phenotype 20-22. Like terminals in lesioned/combinatorially-treated animals, synaptic boutons in intact subjects contained many round synaptic vesicles, made synaptic contacts with single or multiple dendritic targets, and exhibited asymmetric synaptic specializations (Fig. 6e).

In the current study, we did not formally quantify CTB-labeled boutons. However, in equal proportions of tissues scanned ultrastructurally, detection of labeled synapses occurred approximately 30% as frequently in lesioned/combinatorially-treated animals as in intact animals. That is, we identified 6 synapses in approximately 80 fields examined in lesioned/combinatorially-treated subjects, and 10 synapses in approximately 40 fields in intact subjects. Thus, synapse formation in regenerated subjects occurred regularly and was not a rare event.

Electrophysiological Studies

To assess whether synaptic activity could be observed in association with regenerated axons, we recorded extracellularly from the nucleus gracilis in lesioned/combinatorially-treated animals 6 weeks after treatment. To establish a paradigm for recording postsynaptic potentials from the nucleus gracilis, we sampled 20-50 sites throughout the nucleus gracilis in intact subjects for detection of activity following electrical stimulation of the sciatic nerve (Fig. 7a,b). Evoked responses were readily detected in three intact animals, and in three animals without C1 lesions that received conditioning lesions six weeks prior to recording. The number of sites wherein responses could be evoked, and the overall magnitude of the evoked responses comparing intact and sciatic nerve-conditioned animals (Fig. 7c),

indicated that conditioning lesions did not affect the ability to elicit an evoked response. Local application of the glutamate antagonist kynurenic acid nearly abolished evoked responses, and responses returned to near baseline levels after washout of kynurenic acid, indicating that responses were synaptically mediated. (Fig. 7a,b). In addition, in intact animals, subsequent transection of the dorsal columns at thoracic level 3 (T3) completely abolished evoked responses within the nucleus gracilis, indicating that recorded potentials were transmitted through the dorsal columns (Fig. 7a,b). In C1-injured animals, detection of afferent volleys just caudal to the C1 lesion indicated that the intact portions of ascending sensory axons transmitted responses to sciatic nerve stimulation up to the level of the lesion.

Next, we compared responses in intact animals to responses in C1-injured animals that underwent treatment with cell grafts, conditioning lesions and high titer NT-3 (Lenti-NT-3 high+CL; n=5) or GFP vector injections (Lenti-GFP high+CL; n=3) into the nucleus gracilis (Fig. 7c). Because histological analysis showed that GFP vector delivery did not support axonal growth into the nucleus gracilis, we used the maximum root mean square (RMS) response recorded in the lenti-GFP control group as a threshold for analyzing responses in intact and NT-3-treated animals to determine whether responses at individual recording sites exceeded the background response. Postsynaptic potentials in intact animals exceeded the threshold response at 67% of recording sites sampled. In contrast, among animals treated with Lenti-NT-3 high+CL, only two responses, representing 1.4% of recording sites, exceeded those of GFP control animals. Response curves associated with these two sites did not qualitatively differ from those of GFP control animals, nor did they resemble postsynaptic potentials observed in intact animals (Fig. 7d). Thus, combinatorial interventions did not result in detectable post-synaptic potentials within the target in the regions sampled.

Given the fact that combinatorial treatment restored the number of axonal profiles in the nucleus gracilis to 27% of intact values, and that ultrastructural analysis readily revealed synapses in the target tissue, we explored whether factors besides limited sampling of the nucleus gracilis might account for the absence of detectable synaptic activity. In particular, previous studies indicate that demyelinated dorsal column axons fail to sustain efficient conductivity 23, 24. Using double labeling for myelin associated glycoprotein (MAG) and the dorsal column tracer CTB, we confirmed that ascending dorsal column sensory axons projecting toward the lesion site retain myelin sheaths (Fig. 7e). However, CTB-labeled axons regenerating into and *beyond* the lesion site remained unmyelinated or sparsely myelinated (Fig. 7f,g). These findings provide a potential mechanism to account for the lack of detectable synaptic activity in combinatorially-treated subjects, despite extensive axonal regeneration into the nucleus gracilis and the presence of readily-detectable synapses.

Lesion Completeness

Criteria to assess lesion completeness included: 1) disruption of GFAP labeling at all dorso-ventral levels through the graft/lesion site, 2) distinct tissue architecture indicative of cell graft throughout the graft/lesion site under phase contrast optics, and 3) lack of bridges of spared tissue within the lesion in all serial sagittal sections examined by GFAP and phase contrast analysis. Using these criteria, we excluded three animals from the Lenti-

NT-3+NoCL group and one animal from the Lenti-NT-3+CL group; these subjects were not included in the stated numbers per group above. Although we did not observe clearly spared axons in these animals, we could not confirm a complete absence of bridging GFAP immunoreactive tissue in these subjects, and to employ the most conservative criteria, eliminated the subjects from further consideration.

DISCUSSION

Mechanisms that underlie axon growth and directional guidance during neural development have been extensively studied, yielding evidence that chemotropic gradients of growth factors exert an important role in axonal target finding, dendritic growth, and terminal synapse formation 25-29. Studies that examine mechanisms underlying axon growth and potential target-finding after injury in the adult spinal cord have by necessity been far more limited, because until recently there was only limited success in promoting axonal regeneration beyond lesion sites. Taking advantage of combinatorial strategies for promoting bridging regeneration beyond lesion sites 8, 9, 30 together with the capability to control local concentrations and topographies of administered growth factors in vivo in adult animals, we have identified distinct chemotropic mechanisms underlying axonal regeneration in the injured adult spinal cord. Using methods that achieve chemotropic gradients of growth factors in appropriate and inappropriate targets in vivo, we report for the first time the reinnervation of a normal target, the nucleus gracilis, by lesioned, regenerating spinal cord axons, and the chemotropic dependence of this regeneration.

During neural development, regional patterns of neurotrophin expression exert control over axonal guidance and termination in various regions of the nervous system 31-33, including visual cortex 26, 27, 34, the peripheral nervous system 35, 36, central projections of sensory systems 29, and the vestibular system 37. In the present experiment, we expressed NT-3 in both an appropriate target for regenerating axons, and an inappropriate target, and found that axons extended in a topographical distribution that precisely matched regions of NT-3 expression. Indeed, axons could be drawn to inappropriate regions based upon ectopic NT-3 expression, even bypassing a correct target to grow into an NT-3 source. In the absence of NT-3 expression, axons did not reinnervate the target nucleus. In contrast, increasing NT-3 expression in the target (by increasing NT-3 vector dose) significantly increased regeneration into the appropriate region. Collectively, these findings indicate that NT-3 guided regenerating axons to specific topographies, and that an absence of NT-3 resulted in elimination of regenerating axons. Thus, chemotropic guidance mechanisms observed during neural development may be critical in supporting target reinnervation by regenerating axons in adulthood.

This study is the first to demonstrate reinnervation of a natural brainstem target by regenerating spinal cord axons. While previous studies in models of axonal injury in the brain demonstrated target reinnervation in the visual system 38, hippocampus 39 and nigrostriatal projection 40, mechanisms guiding target reinnervation, including chemotropic gradients established by growth factors, have not previously been addressed. In previous studies, lesions were placed either *within* the appropriate target (e.g., striatum), or bridges for regenerating axons ended within an appropriate target (e.g., direct placement of a sciatic

nerve bridge in the lateral geniculate 41), thereby providing unitary targets rather than a choice between appropriate or inappropriate targets for regenerating axons. In some disease models, and spinal cord injury in particular, innumerable incorrect targets become available to regenerating axons, thus *guidance* of regenerating axons is of paramount importance. We have demonstrated in the present study that axons can be guided to appropriate targets utilizing chemotropic gradients of growth factors expressed in correct regions.

Further, we have demonstrated that axons regenerating into the target form synapses. These synapses exhibited appropriate excitatory features of the pre-injured projection, including asymmetric synaptic specializations and clear rounded vesicles. Axo-dendritic rather than axo-somatic synapses and the presence of multiple synaptic targets arising from single axonal terminal shafts are features consistent with the pre-injured ultrastructural phenotype of the dorsal column nuclei 20. Thus, using ultrastructural criteria, the regenerating axon terminals closely resembled the corresponding synaptic boutons in intact animals.

While axons formed synapses when regenerating into the nucleus gracilis, we did not determine whether axons regenerating into an ectopic target, the reticular formation, also formed synapses. Studies in other systems indicate that axons sprouting into ectopic locations modify functional outcomes, suggesting that they likely form synapses in these regions (e.g.42, 43, 44). For example, chronic constrictive lesions of the sciatic nerve cause spontaneous and ectopic growth of sympathetic axons into dorsal root ganglia, associated with dysesthetic pain that can be prevented by blockade of ectopic axon growth 42. Thus, axons growing into either appropriate (present study) or ectopic 42 targets are likely capable of forming synapses.

An important consideration in any study reporting axonal regeneration is the possibility that spared axons may be mistaken for regenerating axons 45. Several observations suggest that regenerating axons observed in our lesioned animals were not spared. First, we employed conservative criteria to eliminate subjects wherein lesion extent was uncertain, based on observations of two experienced, blinded observers. Further, we observed axons emerging from all levels of the rostral host/graft interface, rather than simply at the most dorsal or ventral parts where spared axons might be expected. In addition, we observed axons in ectopic locations beyond the lesion site, where axons are not found in intact animals. In all cases, axons beyond the lesion grew only within regions of NT-3 expression, a finding that would not be expected had axons been spared. Finally, we did not observe axons within the target region in any animals that received control (GFP) lentiviral vector injections. Together, these observations support the presence of regenerated rather than spared axons in the nucleus gracilis.

While lesioned axons in combinatorially-treated animals could be directed into the target and formed synapses, we did not detect electrophysiological responses in the nucleus gracilis following sciatic nerve stimulation. Since we sampled a relatively small volume of the total structure, the absence of target responsiveness may have resulted from limited sampling. However, intact animals exhibited electrophysiological responses in 67% of sampled sites, and NT-3 high+CL treatment restored the number of axonal profiles in lesioned animals to 27% of those in intact subjects. Thus, if reinnervating axons formed

fully functional synapses, one would predict detection of electrophysiological responses in approximately 18% of sampled sites (67% of 27%) in combinatorially-treated animals.

Alternatively, lack of detectable activity might occur if the majority of regenerating axons failed to form synapses; however, synapses associated with CTB-labeled boutons were readily identifiable at the ultrastructural level in both intact and lesioned/combinatorially-treated animals. Further, synapses in regenerating animals exhibited ultrastructural features of normal synapses, including abundant rounded synaptic vesicles and synaptic specializations, suggesting the synapses could be functional. Importantly, however, we found that CTB-labeled regenerating dorsal column sensory axons emerging from the lesion site were either unmyelinated or poorly myelinated, in contrast to the intact state of these projections 46. Demyelination of dorsal column sensory projections leads to conduction failure 23. While it is possible that remyelination might have occurred after the six week time point at which we assessed electrophysiological activity, a recent report indicated a persistent loss of dorsal column sensory axon myelination in the thoracic spinal cord even six months after regeneration induced by anti-NG2 and conditioning lesions 24. Further, spontaneous remyelination of injured host axons after spinal cord injury is reportedly unstable, falling over extended time periods post-lesion 47. Persistent demyelination is therefore a candidate mechanism for the lack of synaptic activity observed in the present study. Thus, *despite* the demonstration that conditioning of the injured neuron together with chemotropic guidance can direct regenerating central axons to form synaptic contacts with appropriate gracilar targets, synaptic activity was not restored.

To our knowledge this is the first direct observation of a concept that has been previously advanced but not proven: that comprehensive attempts to restore functional neural circuitry after spinal cord injury must address not only axonal growth and target location, but remyelination. It is not likely that regenerated axons will be functional unless action potentials can be efficiently transmitted through regenerated segments. Our studies highlight the complexities of restoring function, and provide a model system in which these complexities can be further explored.

In summary, we demonstrate a tropic dependency for target reinnervation, and evidence for supraspinal target reinnervation after combinatorial application of therapies to the injured adult CNS. Progress in understanding mechanisms of appropriate axon guidance and termination is of critical importance in the field of CNS regeneration, as experimental strategies that enhance axonal growth after injury in the adult CNS continue to be identified. Axons face far more inappropriate than appropriate targets when extending beyond lesion sites after spinal cord injury, and the elucidation of mechanisms that guide directional growth into appropriate targets is essential. The present study identifies chemotropic guidance as an important mechanism that can guide regenerating axons into appropriate targets and lead to synapse formation.

METHODS

Production of lentiviral vectors and isolation of marrow stromal cells (MSCs)

NT-3 and control (GFP-expressing) lentiviral plasmids were constructed as previously described 10. The NT-3 virus construct contains a GFP expression cassette 48. Vector titers were assayed by infection of 293 cells and quantification of p24 levels as previously described 10. NT-3 vector preparations were diluted to 100 or 200 $\mu\text{g/ml}$ p24 (8.3×10^7 or 1.7×10^8 IU/ml) before injection. Rat primary marrow stromal cells were isolated from tibias and femurs, as previously described 49. Briefly, tibias and femurs were dissected and bone marrow extruded. Cells were cultured in alpha-MEM medium (Invitrogen, Carlsbad, CA) supplemented with 20% fetal bovine serum (FBS) and antibiotics.

Surgical procedures

Adult female Fischer 344 rats weighing 150-200 gm were used. Institutional, NIH, and Society for Neuroscience guidelines on animal care were followed. Animals were anesthetized with a combination (2 ml/kg) of ketamine (25 mg/ml), xylazine (1.3 mg/ml) and acepromazine (0.25 mg/ml). One week before spinal cord lesion surgery, gracilar neurons were retrogradely labeled by injections of Fluorogold into the ventroposterolateral (VPL) nucleus of the thalamus (Fig. 1). A solution of 4% fluorogold in 0.9% sterile saline was delivered stereotactically to 12 sites (6 per hemisphere, approximately 80 nl/site) using 20 μm diameter pulled glass pipettes and pressure injection. Measurements relative to Bregma: coordinates #1-3: -0.23 rostro-caudal (R/C), 0.30 mediolateral (M/L), and 0.49, 0.56, 0.62 dorso-ventral (D/V); coordinate #4: -0.30 (R/C), 0.30 (M/L), 0.61 (D/V); coordinate #5: -0.30 (R/C), 0.34 (M/L), 0.53 (D/V); coordinate #6: -0.36 (R/C), 0.34 (M/L), 0.58 (D/V). Immediately following retrograde labeling, some animals received bilateral conditioning lesions, in which the sciatic nerve was crushed at mid-thigh level with a jeweler's forceps for 15 seconds. For C1 lesion and vector injections, animals were fixed in a spinal stereotaxic unit and a partial laminectomy was performed to remove the rostral half of the C1 vertebrae. Dorsal column lesions were made 1.5 mm caudal to the obex using a Kopf microwire device (Kopf Instruments, Tujunga, CA). The wire knife was lowered 0.5 mm into the spinal cord at a position 1.25 mm to the left of the midline. Extrusion of the wireknife formed a 2.5 mm-wide arc that was raised to the dorsal surface of the cord, transecting the ascending (sensory) axon tracts..

Immediately following the lesion, 2 μl (75,000 cells/ μl) of marrow stromal cells (MSC) were pressure injected (Picospritzer II, General Valve, Fairfield, NJ) through a small hole in the dura mater into the lesion space. Next, lentiviral vectors were pressure injected through pulled glass capillaries 1.75 mm rostral to the C1 lesion site into the rostral portion of the nucleus gracilis and reticular nucleus bilaterally (1.25 $\mu\text{l}/\text{side}$) or into the nucleus gracilis alone. Injections targeting the nucleus gracilis and reticular nucleus distributed vector primarily at depths spanning 0.25-0.5 mm and 1.0 mm below the dorsal brainstem surface, respectively. 4 weeks after injury/treatment surgery, animals received injections of cholera toxin B subunit (CTB, 1%; 2 μl , List Biologicals; Campbell, CA) into the right and left sciatic nerves to label ascending sensory projections transganglionically. Three days later,

animals were perfused with either 4% paraformaldehyde (histology/immunocytochemistry) or 4% paraformaldehyde plus 2.5% glutaraldehyde (electron microscopy).

Immunohistochemical analysis of brainstem sections

For immunohistochemical analysis, every 6th 35 μ m-thick section was labeled for CTB using streptavidin-HRP light level immunohistochemistry followed by GFP and GFAP fluorescent immunolabeling as previously described 10. Antibodies to CTB (goat anti-CTB 1:80,000; List, Campbell, CA) were used to detect ascending sensory axons, to glial fibrillary acidic protein (GFAP, monoclonal 1:1000; Chemicon, Temecula, CA) to label astrocytes and to green fluorescent protein (rabbit anti-GFP 1:750; Molecular Probes, Eugene, OR) to label vector-transduced cells as previously described 10. For confocal analysis, double immunofluorescent labeling of CTB and fluorogold was performed using a 3-day incubation at 4°C in primary antibodies (rabbit anti-fluorogold 1:2000; Chemicon, goat anti-CTB 1:20,000) followed by fluorescent-conjugated secondary antibody incubation. For double immunofluorescent labeling of CTB and myelin associated glycoprotein (MAG), sections were incubated for 3 days at 4°C in primary antibodies (goat anti-CTB 1:10,000 and mouse anti-MAG 1:250; Millipore, Billerica, MA) followed by incubation with fluorescent conjugated secondary antibodies. Brainstem sections were labeled for NT-3 using streptavidin-HRP light level immunohistochemistry, as previously described 10 with a 2-day primary antibody incubation at 4°C (goat anti-NT-3, Neuromics, GT15000, 1:1000).

Animal exclusion criteria

Lesions were considered potentially incomplete based on highly conservative criteria: an animal was excluded if examination of every 6th 35 μ m-thick section immunolabeled for GFAP indicated an incomplete interruption of GFAP-labeled astrocytes at the lesion site, in particular at the most dorsal aspect, or if tissue architecture anywhere within the lesion site resembled host tissue rather than grafted cells. Based on these criteria, animals in the following groups were excluded: n=3, Lenti-NT-3 + noCL; n=1, Lenti-NT-3 + CL. Animal numbers stated in Results are the final number of animals included per group.

Quantification of axon profiles in the nucleus gracilis

Axon profiles in the nucleus gracilis were quantified using StereoInvestigator software (Microbrightfield, Williston, VT). In a series of every 6th 35 μ m thick section, the three most medial sections were selected for analysis by an observer blinded to group identity. For each section, the nucleus gracilis was outlined and overlaid with a point grid consisting of crosses (+) spaced 25 μ m apart and placed at a randomized angle. Each grid point that was intersected by a CTB-labeled axon was counted. The number of grid points with intersections were then divided by the total number of grid points in the nucleus gracilis to determine percent axon intersections (grid points with axon intersections/total grid points). Percent axon intersections in three quantified sections per animal were compared between groups.

Electron microscopic analysis of brainstem sections

Two animals that received combined treatment with conditioning lesions and high titer lenti-NT-3 vector injection into the nucleus gracilis, and three intact animals, were used for electron microscopy, as previously described 50. Briefly, after CTB/GFAP immunohistochemical labeling of one series of 1-in-6 sections to verify lesion completeness, adjacent sections were immunolabeled for CTB. 2-3 of these sections per animal were prepared for EM analysis by osmication in 1% osmium tetroxide, dehydration, embedding in Durcupan® ACM (Electron Microscopy Sciences, Fort Washington, PA), and sandwiching between Aclar embedding films. Ultrathin sections (60-70 nm) were serially collected on formvar-coated copper one-hole grids, counterstained with uranyl acetate and lead citrate, and fields were examined at a screening magnification of 4800x in a JEOL 100 CX electron microscope. 2-5 ultrathin sections were examined per animal for evidence of CTB-labeled synaptic structures. Approximately 80 fields were examined in lesioned subjects, and 40 fields in intact subjects.

Electrophysiology

Electrophysiological recordings were collected from the nucleus gracilis after sciatic nerve stimulation. Measurements were made in: 1) intact animals (n=3), 2) animals with intact spinal cords but crushed (conditioned) sciatic nerves (n=3), 3) animals with C1 dorsal column lesions, conditioning lesions, cell grafts, and high titer lenti-NT-3 injections to the nucleus gracilis (Lenti-NT-3 high + CL, n=5); and 4) animals with C1 dorsal column lesions, conditioning lesions, cell grafts, and high titer lenti-GFP injections into the target (Lenti-GFP high + CL, n=3). Data were obtained 6 weeks after lesion/treatment from urethane-anesthetized rats (1.2-1.6 g/kg, i.p.). Wire electrodes for stimulation were hooked around sciatic nerves bilaterally. Animals were then secured in a precision stereotax and glass microelectrodes (1-3 M ohm impedance) filled with 3M NaCl were used to obtain extracellular recordings from the ipsilateral nucleus gracilis. Recordings were made at regular intervals beginning 200 μ m rostral through 1400 μ m caudal to the obex; 500 μ m mediolateral of the midline; and through a range of 100-500 μ m below the dorsal surface of the brainstem. The sciatic nerve was stimulated at 20 second intervals using a current of 1.0 mA. The magnitude of nucleus gracilis unit responses were quantified over a 10 msec window, beginning 6.0 msec after the stimulus onset, by calculating the root mean square of the waveform. Each post stimulus value was normalized by subtracting the RMS values calculated from a 10 msec window ending 6 msec before the stimulus onset. This method of analysis yielded a single numerical value for the response that was normalized to the pre-stimulus baseline gracilis activity at each recording site. For each recording site, several responses were recorded and the average RMS response was determined. The maximum RMS response observed in lesioned animals lacking regenerated axons (Lenti-GFP high + CL group) was used as a minimum threshold to categorize responses. Responses below the control max response were considered negative and those above it were considered positive. To verify that evoked responses were due to synaptic activation, the response to pharmacological blockade of glutamatergic transmission using kynurenic acid was determined. Additional verification that evoked responses were mediated by axons in the dorsal columns was obtained by comparing responses before and after a transection of the dorsal columns at spinal cord level T2.

Statistics

Comparisons of axon density in groups treated with identical doses of lentiviral vectors were assessed by Kruskal-Wallis with posthoc Dunn's; non-parametric tests were used because some groups lacked bridging axons and data were non-normally distributed. Subsequent comparisons of axon density between high and low dose viral vector groups (Lenti-NT-3 high + CL and Lenti-NT-3 + CL) were made using a two-tailed t-test because data were normally distributed. Comparison of vector spread in the target was made by ANOVA with post-hoc Fisher's. To compare reinnervation after NT-3 treatment to normal innervation, ANOVA followed by Dunnet's posthoc tests was used. Electrophysiological responses in spinally intact animals were compared using repeated measures ANOVA with posthoc Fisher's. A significance criterion of $p < 0.05$ was used in all statistical tests.

Supplementary Material

Refer to Web version on PubMed Central for supplementary material.

ACKNOWLEDGMENTS

We thank Lawrence Ma and Birgitta Sjöstrand for technical assistance, and Jerry Silver for helpful suggestions. Supported by the National Institutes of Health (NS09881; NS 54883), the Veterans Administration, the International Spinal Research Trust, Wings for Life, the Dr. Miriam and Sheldon G. Adelson Medical Research Foundation, and the Bernard and Anne Spitzer Charitable Trust.

REFERENCES

1. McQuarrie IG, Grafstein B, Gershon MD. Axonal regeneration in the rat sciatic nerve: effect of a conditioning lesion and of dbcAMP. *Brain Res.* 1977; 132:443–453. [PubMed: 199316]
2. Schreyer DJ, Skene JH. Injury-associated induction of GAP-43 expression displays axon branch specificity in rat dorsal root ganglion neurons. *J Neurobiol.* 1993; 24:959–970. [PubMed: 8228973]
3. Chen DF, Schneider GE, Martinou JC, Tonegawa S. Bcl-2 promotes regeneration of severed axons in mammalian CNS. *Nature.* 1997; 385:434–439. [PubMed: 9009190]
4. Goldberg JL, Klassen MP, Hua Y, Barres BA. Amacrine-signaled loss of intrinsic axon growth ability by retinal ganglion cells. *Science.* 2002; 296:1860–1864. [PubMed: 12052959]
5. Yiu G, He Z. Glial inhibition of CNS axon regeneration. *Nat Rev Neurosci.* 2006; 7:617–627. [PubMed: 16858390]
6. Schnell L, Schwab ME. Axonal regeneration in the rat spinal cord produced by antibody against myelin-associated neurite growth inhibitors. *Nature.* 1990; 343:269–272. [PubMed: 2300171]
7. Bradbury EJ, et al. Chondroitinase ABC promotes functional recovery after spinal cord injury. *Nature.* 2002; 416:636–640. [PubMed: 11948352]
8. Lu P, Yang H, Jones LL, Filbin MT, Tuszynski MH. Combinatorial therapy with neurotrophins and cAMP promotes axonal regeneration beyond sites of spinal cord injury. *J Neurosci.* 2004; 24:6402–6409. [PubMed: 15254096]
9. Pearse DD, et al. cAMP and Schwann cells promote axonal growth and functional recovery after spinal cord injury. *Nat Med.* 2004; 10:610–616. [PubMed: 15156204]
10. Taylor L, Jones L, Tuszynski MH, Blesch A. Neurotrophin-3 gradients established by lentiviral gene delivery promote short-distance axonal bridging beyond cellular grafts in the injured spinal cord. *J Neurosci.* 2006; 26:9713–9721. [PubMed: 16988042]
11. Thuret S, Moon LD, Gage FH. Therapeutic interventions after spinal cord injury. *Nat Rev Neurosci.* 2006; 7:628–643. [PubMed: 16858391]
12. Hofstetter CP, et al. Marrow stromal cells form guiding strands in the injured spinal cord and promote recovery. *Proc Natl Acad Sci.* 2002; 99:2199–2204. [PubMed: 11854516]

13. Qiu J, et al. Spinal axon regeneration induced by elevation of cyclic AMP. *Neuron*. 2002; 34:895–903. [PubMed: 12086638]
14. Richardson PM, Issa VM. Peripheral injury enhances central regeneration of primary sensory neurones. *Nature*. 1984; 309:791–793. [PubMed: 6204205]
15. Neumann S, Woolf CJ. Regeneration of dorsal column fibers into and beyond the lesion site following adult spinal cord injury. *Neuron*. 1999; 23:83–91. [PubMed: 10402195]
16. Neumann S, Bradke F, Tessier-Lavigne M, Basbaum AI. Regeneration of sensory axons within the injured spinal cord induced by intraganglionic cAMP elevation. *Neuron*. 2002; 34:885–893. [PubMed: 12086637]
17. Nieuwenhuys R. The neocortex. An overview of its evolutionary development, structural organization and synaptology. *Anat Embryol (Berl)*. 1994; 190:307–337. [PubMed: 7840420]
18. Garner CC, Zhai RG, Gundelfinger ED, Ziv NE. Molecular mechanisms of CNS synaptogenesis. *Trends Neurosci*. 2002; 25:243–251. [PubMed: 11972960]
19. Peters A, Palay SL. The morphology of synapses. *J Neurocytol*. 1996; 25:687–700. [PubMed: 9023718]
20. De Biasi S, Vitellaro-Zuccarello L, Bernardi P, Valtchanoff JG, Weinberg RJ. Ultrastructural and immunocytochemical characterization of primary afferent terminals in the rat cuneate nucleus. *J Comp Neurol*. 1994; 347:275–287. [PubMed: 7814668]
21. Hwang SJ, Rustioni A, Valtchanoff JG. Kainate receptors in primary afferents to the rat gracile nucleus. *Neurosci Lett*. 2001; 312:137–140. [PubMed: 11602329]
22. Rustioni A, Sotelo C. Synaptic organization of the nucleus gracilis of the cat. Experimental identification of dorsal root fibers and cortical afferents. *J Comp Neurol*. 1974; 155:441–468. [PubMed: 4847733]
23. Kohama I, et al. Transplantation of cryopreserved adult human Schwann cells enhances axonal conduction in demyelinated spinal cord. *J Neurosci*. 2001; 21:944–950. [PubMed: 11157080]
24. Tan AM, Petruska JC, Mendell LM, Levine JM. Sensory afferents regenerated into dorsal columns after spinal cord injury remain in a chronic pathophysiological state. *Exp Neurol*. 2007; 206:257–268. [PubMed: 17585905]
25. Letourneau PC. Chemotaxic response of nerve fiber elongation to nerve growth factor. *Dev. Biol*. 1978; 66:183–196. [PubMed: 751835]
26. Cabelli RJ, Hohn A, Shatz CJ. Inhibition of ocular dominance column formation by infusion of NT-4/5 or BDNF. *Science*. 1995; 267:1662–1666. [PubMed: 7886458]
27. McAllister AK, Katz LC, Lo DC. Opposing roles for endogenous BDNF and NT-3 in regulating cortical dendritic growth. *Neuron*. 1997; 18:767–778. [PubMed: 9182801]
28. Ma L, et al. Neurotrophin-3 is required for appropriate establishment of thalamocortical connections. *Neuron*. 2002; 36:623–634. [PubMed: 12441052]
29. Genc B, Ozdinler PH, Mendoza AE, Erzurumlu RS. A chemoattractant role for NT-3 in proprioceptive axon guidance. *PLoS Biol*. 2004; 2:e403. [PubMed: 15550985]
30. Houle JD, et al. Combining an autologous peripheral nervous system "bridge" and matrix modification by chondroitinase allows robust, functional regeneration beyond a hemisection lesion of the adult rat spinal cord. *J Neurosci*. 2006; 26:7405–7415. [PubMed: 16837588]
31. Gunderson RW, Barrett JN. Characterization of the turning response of dorsal root neurites toward nerve growth factor. *J. Cell Biol*. 1980; 87:546–554. [PubMed: 6257725]
32. Arévalo JC, Chao MV. Axonal growth: where neurotrophins meet Wnts. *Curr Opin Cell Biol*. 2005; 17:112–115. [PubMed: 15780585]
33. Markus A, Patel TD, Snider WD. Neurotrophic factors and axonal growth. *Curr. Opin. Neurobiol*. 2002; 12:523–531. [PubMed: 12367631]
34. Cohen-Cory S, Fraser S. Effects of brain-derived neurotrophic factor on optic axon branching and remodelling in vivo. *Nature*. 1995; 378:192–196. [PubMed: 7477323]
35. Zhang L, Schmidt RE, Yan Q, Snider WD. NGF and NT-3 have differing effects on the growth of dorsal root axons in developing mammalian spinal cord. *J Neurosci*. 1994; 14
36. Postigo A, et al. Distinct requirements for TrkB and TrkC signaling in target innervation by sensory neurons. *Genes Dev*. 2002; 16:633–645. [PubMed: 11877382]

37. Tessarollo L, Coppola V, Fritsch B. NT-3 replacement with brain-derived neurotrophic factor redirects vestibular nerve fibers to the cochlea. *J Neurosci.* 2004; 24:2575–2584. [PubMed: 15014133]
38. Vidal-Sanz M, Bray GM, Villegas-Perez MP, Thanos S, Aguayo A. Axonal regeneration and synapse formation in the superior colliculus by retinal ganglion cells in the adult rat. *J. Neurosci.* 1987; 7:2894–2907. [PubMed: 3625278]
39. Tuszynski MH, Gage FH. Bridging grafts and transient NGF infusions promote long-term CNS neuronal rescue and partial functional recovery. *Proc. Nat. Acad. Sci.* 1995; 92:4621–4625. [PubMed: 7753852]
40. Moon LD, Asher RA, Rhodes KE, Fawcett JW. Regeneration of CNS axons back to their target following treatment of adult rat brain with chondroitinase ABC. *Nat Neurosci.* 2001; 4:465–466. [PubMed: 11319553]
41. Keirstead SA, Rasminsky M, Fukuda Y, Carter D, Aguayo AJ. Electrophysiologic responses in hamster superior colliculus evoked by regenerating retinal axons. *Science.* 1989; 246:255–258. [PubMed: 2799387]
42. Ramer MS, Bisby MA. Adrenergic innervation of rat sensory ganglia following proximal or distal painful sciatic neuropathy: distinct mechanisms revealed by anti-NGF treatment. *Eur J Neurosci.* 1999; 11:837–846. [PubMed: 10103077]
43. Zhou XF, Deng YS, Xian CJ, Zhong JH. Neurotrophins from dorsal root ganglia trigger allodynia after spinal nerve injury in rats. *Eur J Neurosci.* 2000; 12:100–105. [PubMed: 10651864]
44. Dancause N, et al. Extensive cortical rewiring after brain injury. *J Neurosci.* 2005; 25:10167–10179. [PubMed: 16267224]
45. Steward O, Zheng B, Tessier-Lavigne M. False resurrections: distinguishing regenerated from spared axons in the injured central nervous system. *J Comp Neurol.* 2003; 459:1–8. [PubMed: 12629662]
46. LaMotte CC, Kapadia SE, Shapiro CM. Central projections of the sciatic, saphenous, median, and ulnar nerves of the rat demonstrated by transganglionic transport of cholera toxin B-subunit (B-HRP) and wheat germ agglutinin-HRP (WGA-HRP). *J Comp Neurol.* 1991; 311:546–562. [PubMed: 1721924]
47. Totoiu MO, Keirstead HS. Spinal cord injury is accompanied by chronic progressive demyelination. *J Comp Neurol.* 2005; 486:373–383. [PubMed: 15846782]
48. Naldini L, et al. In vivo gene delivery and stable transduction of nondividing cells by a lentiviral vector. *Science.* 1996; 272:263–267. [PubMed: 8602510]
49. Azizi SA, Stokes D, Augelli BJ, DiGirolamo C, Prockop DJ. Engraftment and migration of human bone marrow stromal cells implanted in the brains of albino rats--similarities to astrocyte grafts. *Proc Natl Acad Sci U S A.* 1998; 95:3908–3913. [PubMed: 9520466]
50. Havton LA, Broman J. Systemic administration of cholera toxin B subunit conjugated to horseradish peroxidase in the adult rat labels preganglionic autonomic neurons, motoneurons, and select primary afferents for light and electron microscopic studies. *J Neurosci Methods.* 2005; 149:101–109. [PubMed: 16054225]

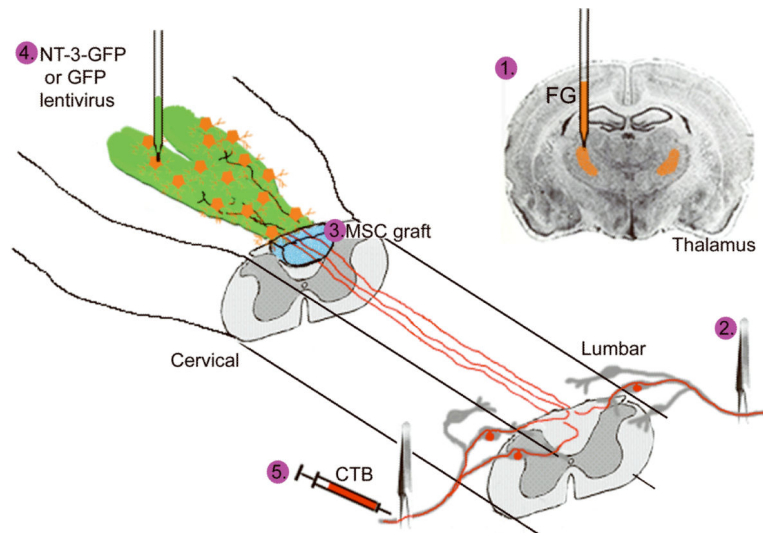


Figure 1. Experimental paradigm

1) Nucleus gracilis neurons were retrogradely labeled using bilateral injection of fluorogold (FG, orange) into the ventro-postero-lateral (VPL) thalamus one week prior to dorsal column lesions. **2)** Some animals received bilateral sciatic nerve conditioning lesions, while controls received no sciatic nerve lesions. **3)** 7 days later a wire knife was used to transect the dorsal columns approximately 1.5 mm caudal to the obex, and marrow stromal cells (MSCs) were grafted into the lesion site. **4)** Immediately after grafting, lentiviral vectors expressing both NT-3 and GFP (“Lenti-NT-3”, GFP is expressed from an internal ribosome entry site [IRES] in the same construct) or GFP alone (“Lenti-GFP”) were injected into the nucleus gracilis and median reticular nucleus bilaterally, slightly rostral and lateral to the obex, or to the nucleus gracilis alone. **5)** 4 weeks later, ascending sensory tracts were bilaterally labeled using cholera toxin B subunit (CTB) injections into the sciatic nerve; 3 days after CTB injections, animals were perfused.

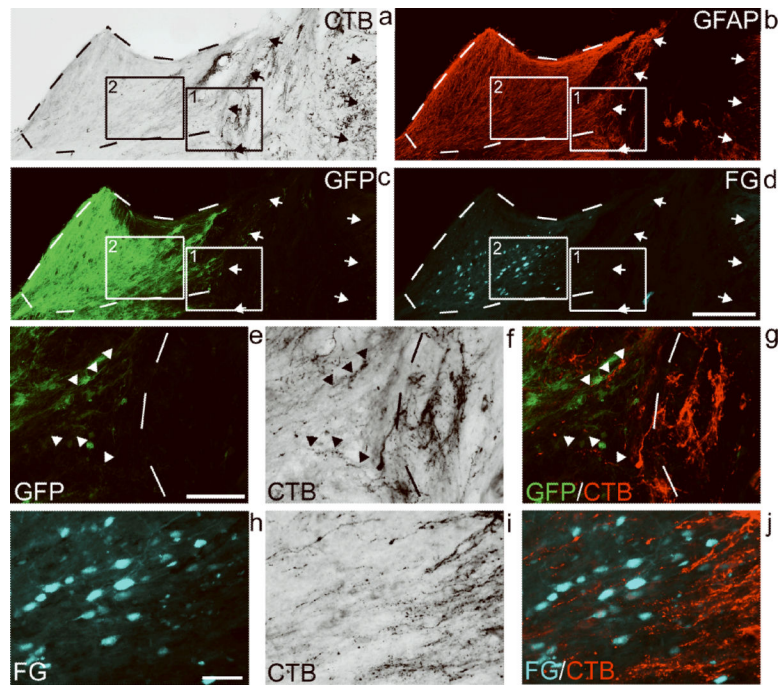


Figure 2. Transected ascending sensory axons extend toward Lenti-NT-3-transduced cells in the denervated nucleus gracilis

Multiple labeling for (a) CTB to identify ascending sensory axons, (b) GFAP to indicate the lesion/graft borders (arrows), (c) GFP to identify NT-3-GFP vector-transduced cells, and (d) fluorogold (FG) fluorescence to identify nucleus gracilis neurons, in a sagittal lower medulla/spinal cord section 4 weeks after dorsal column lesion, cell grafting and lenti-NT-3 gene delivery (200 µg/ml) to the nucleus gracilis (Lenti-NT-3 high+CL group). Dashed lines encircle the nucleus gracilis. Boxes 1 and 2 are shown at higher magnification in **e-g** and **h-j**, respectively. (e) In a region containing NT-3-GFP expression at the rostral graft/host border, (f) CTB-labeled axons cross the lesion border (dashed lines) into rostral host tissue. (g) Merge of **e** and **f** with CTB-labeled axons pseudo-colored in red. (h) Regions of NT-3-GFP expression overlap with regions containing FG-labeled nucleus gracilis neurons, and (i) CTB-labeled axons are present in these regions. (j) Merge of **h** and **i** with axons pseudo-colored in red. Scale bars: d, 250 µm; e, 100 µm; f, 50 µm.

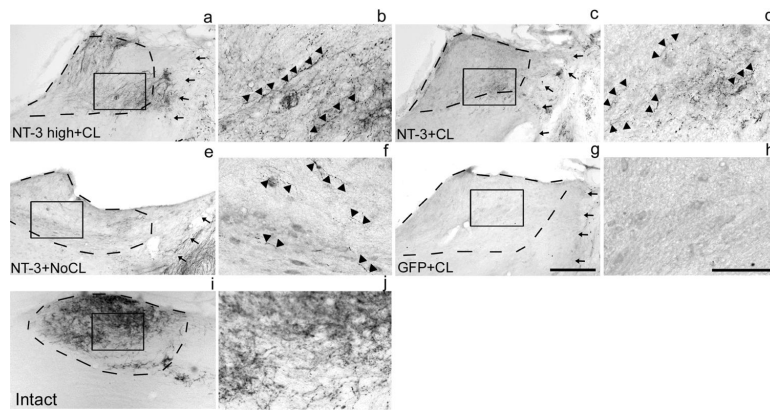


Figure 3. Comparison of axon growth into the nucleus gracilis after viral GFP or NT-3 delivery with or without conditioning lesions

(a-f) Axons were observed regenerating beyond the rostral lesion border (arrows) and into the nucleus gracilis (dashed lines) in animals that received (a,b) high titer NT-3 virus delivered to the nucleus gracilis plus conditioning lesions (Lenti-NT-3 high+CL group); (c,d) standard titer NT-3 virus delivered to the gracile and reticular nuclei plus conditioning lesions (Lenti-NT-3+CL group); and (e,f) standard titer NT-3 virus delivered to the gracile and reticular nuclei without conditioning lesions (Lenti-NT-3+NoCL group). The greatest number of axons was observed in animals with combinatorial treatment (a-d), and among these 2 groups, more axons were observed when (a,b) high titer NT-3 virus was delivered to the nucleus gracilis (See Fig. 4). In contrast, no axons were observed within the nucleus gracilis in animals that received (g,h) GFP lentivirus delivery plus conditioning lesions (Lenti-GFP+CL group), or GFP lentivirus alone (Lenti-GFP+NoCL, not shown). (i,j) Innervation in the intact nucleus gracilis is shown for comparison. Panels b,d,f and h and j are high magnification of boxes in panels a,c,e,g and i, respectively. Axons are indicated by arrowheads. Nucleus gracilis outlines (dashed lines) were established using Fluorogold fluorescence. Scale bars: g, 250 μ m; h, 100 μ m.

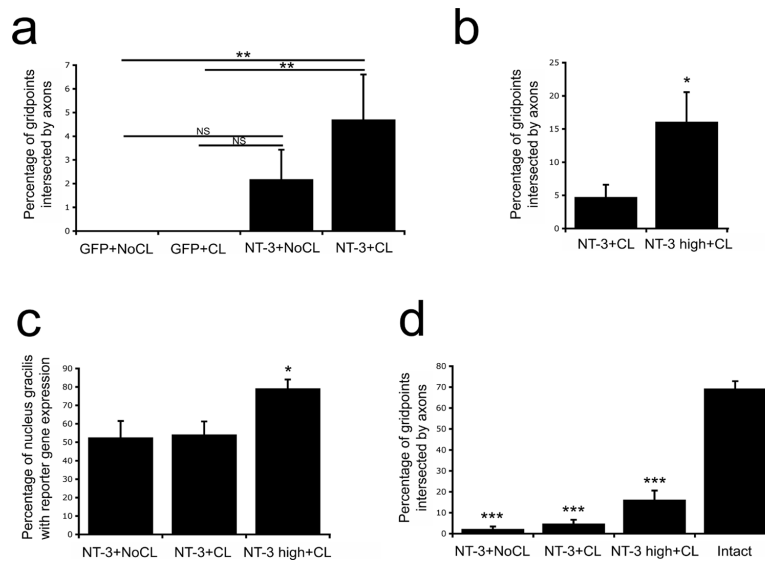


Figure 4. Quantification of CTB-labeled axons and reporter gene expression in the nucleus gracilis

(a) CTB-labeled axonal profiles within the nucleus gracilis were observed only in subjects that received lenti-NT-3 injections. The combination of lenti-NT-3 injections and conditioning lesions (NT-3+CL) elicited significantly greater axon growth into the target nucleus than control groups that received GFP-expressing vectors (GFP+CL and GFP+NoCL, Kruskal-Wallis $p=0.0003$, posthoc Dunn's, $**p<0.01$). Axon density among subjects that received lenti-NT-3 alone, without conditioning lesions (NT-3+No CL), did not differ significantly from GFP controls (NS). (b) Animals that received higher dose NT-3 vector (NT-3 high+CL) had significantly more regenerating axons in the nucleus gracilis than subjects treated with the lower “standard” vector dose (NT-3+CL, two-tailed t test, $*p<0.05$). (c) The proportion of the nucleus gracilis exhibiting reporter gene (GFP) expression was significantly higher in animals that received high titer lenti-NT-3 virus compared to animals that received a standard titer NT-3 vector dose (ANOVA, $p=0.03$, Fisher's PLSD, $*p<0.05$). (d) Axon density after NT-3 treatment was significantly lower than normal innervation of the nucleus gracilis (ANOVA, $p<0.0001$, Dunnett's posthoc test comparing all injured/treated groups to intact animals, $***p<0.001$), but NT-3 high+CL treatment restored 27% of pre-injury axon density. Values are mean \pm s.e.m. CL, conditioning lesion; NT-3 high, 200 μ g/ml lenti-NT-3 vector.

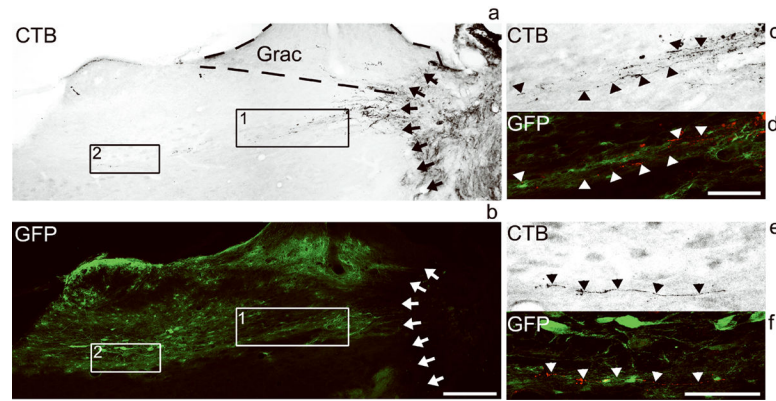


Figure 5. Lesioned axons regenerate to ectopic regions when NT-3 is ectopically expressed
(a) CTB-labeled axons regenerate into the medullary reticular nucleus (boxes) when **(b)** lenti-NT-3 virus is injected into this ectopic location. Dashed lines encircle the nucleus gracilis (Grac). Boxes 1 and 2 are shown at high magnification in **c,d** and **e,f**, respectively. **(c,e)** Ectopic axons extend into regions of **(d,f)** NT-3 expression, indicated by the reporter gene GFP. CTB labeled axons are pseudo-colored in red in **d** and **f**. Scale bars: b, 250 μ m; c,d, 100 μ m.

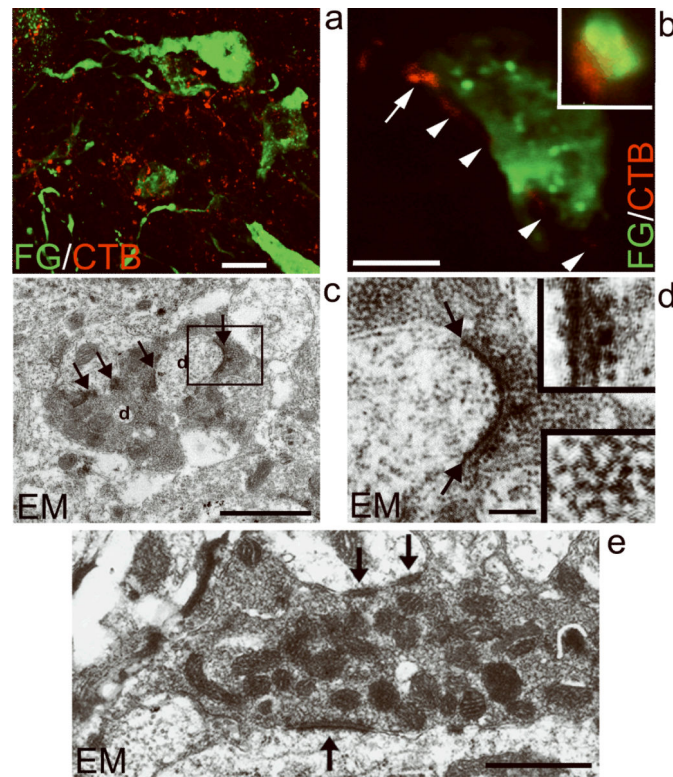


Figure 6. Regenerating axons form new synapses in the denervated nucleus gracilis

(a) A confocal stack shows many CTB-labeled axons (red) in close proximity to FG-labeled target neurons (green) in nucleus gracilis in an animal that received NT-3 high+CL treatment. (b) A single plane confocal image indicates close apposition of a CTB-labeled axon (arrowheads) to a FG-labeled dendrite (green); arrow indicates a bouton-like structure. Inset in single confocal plane shows intimate association between a CTB-labeled axon and FG-labeled target dendrite. (c) A CTB-labeled bouton in the nucleus gracilis of an animal that also received NT-3 high+CL treatment is identified under the electron microscope by the electron-dense reaction product produced by CTB immunohistochemistry. Multiple synaptic specializations are present (arrows), and dendritic processes (d) protrude through the axoplasm. (d) High magnification of boxed area in c, highlighting a synaptic contact. The synaptic specialization is asymmetric (top inset); electron dense labeling indicates synaptic vesicles surrounded by the CTB reaction product (bottom inset). (e) The regenerated synapse resembles a CTB-labeled synapse from an intact animal (shown), which is also characterized by multiple synaptic specializations (arrows) and dark background labeling identifying CTB. Scale bars: a, 5 μm ; b, 2.5 μm (inset 3-fold magnification); c, 1 μm ; d, 0.4 μm (insets 5-fold magnification); e, 0.75 μm .

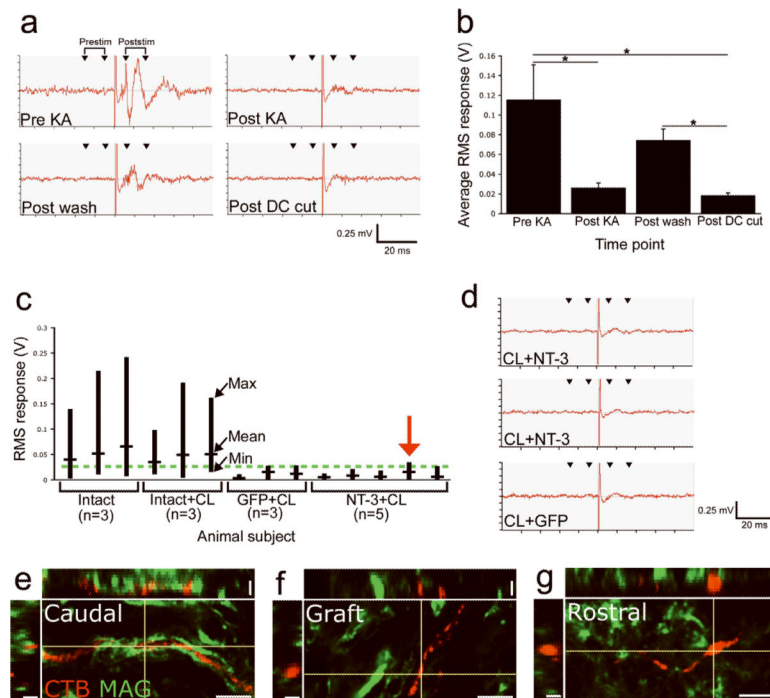


Figure 7. Electrophysiological responses in the nucleus gracilis evoked by sciatic nerve stimulation in intact and C1 injured animals

(a) Representative traces from a single recording site (intact animal). Baseline recordings (Pre KA), after addition of kynurenic acid [$50 \mu\text{M}$] (Post KA), following washout of kynurenic acid with artificial cerebrospinal fluid (Post wash) and after dorsal column transection at T3 (Post DC cut). Arrowheads indicate pre- and post-stimulus windows for calculating root mean square (RMS) power spectrum responses. (b) Average responses ($n=6$ animals). Repeated measures ANOVA $p=0.006$, Fisher's PLSD, $*p<0.05$, mean \pm s.e.m. (c) Responses to sciatic nerve stimulation recorded in the nucleus gracilis in: i) intact animals, ii) intact animals with conditioning lesions (CL), iii) C1 lesioned animals with GFP high +CL treatment, and iv) C1 lesioned animals with NT-3 high+CL treatment. Vertical lines indicate the maximum, minimum and mean RMS response values obtained from all recording sites for individual animals. Green dotted line indicates the maximum RMS response recorded in GFP+CL animals. Responses exceeded the maximum control response at two sites in one NT-3+CL animal (red arrow). (d) However, these recordings did not resemble evoked activity (top 2 traces); responses were comparable to those in GFP-treated control animals (bottom trace). (e) Axons in the intact dorsal columns and axons ascending toward the cervical lesion site (shown) were myelinated, while axons regenerating (f) within and (g) beyond the lesion/graft site in combinatorially treated subjects were not myelinated, as revealed by double labeling for CTB and myelin-associated glycoprotein (MAG).